Stress Intensity Parameter and Crack Growth of Iraqi Hot Mix Asphalt Mixtures

Habil Tom Schanz[1], Zainab Ahmed Abdulsattar[2]

[1]Ruhr-Universität Bochum, Germany

[2]AlMustansiriyah university, Iraq

ABSTRACT— ***The primary objective of this research is to evaluate the fracture toughness and crack propagation. To accomplish the main objectives laboratory tests on fracture parameters of asphalt mixtures are made to evaluate the potential of stress intensity factor and fracture resistance of asphaltic materials. The semi circular bending test (SCB) was carried out to achieve the objectives of this research. It can conclude that the fracture toughness increased as the test temperature decreased, which means that the HMA becomes more brittle at cold temperatures. Also the asphalt mixture with 5% binder content at (0 C^o and 20 C^o) had the highest average K_{IC} value and also decreasing test temperature increased the critical stress intensity factor by (57.5 %). Again it can be concluded that as the temperature decrease, the fracture energy deceases but the fracture toughness increases. Also with decreasing the test temperature, the peak load increases and the total displacement decreases. The obtained results showed that peak load increased by approximately (45.95 %) and the total displacement decreases by (19 %). Also decreasing the test temperature increase the critical mouth opening displacement (CMOD) and asphalt mixture with (5%) binder had the lower critical mouth opening displacement CMOD at unstable crack.***

Keywords— Fracture toughness, Stress intensity factor, Crack, Asphalt mixtures, fracture energy, Temperature effect, Semi circular Test.

1. INTRODUCTION

Traffic loads are repetitive in nature and, therefore, lead to fatigue in the bound layers of the pavement structure. As, a result, one of the design criteria for asphalt concrete roads is fatigue cracking. Fatigue cracks can initiate both at the top and at the bottom of pavement. Cracks that initiate at the top are due to the outward shear stresses caused by the tires. They are influenced by the characteristics of the wearing course (stiffness, roughness), but not by the pavement structure. Cracks that initiate at the bottom are caused by repetitive tensile stress, which are the result of bending of the pavement layers due to passing of wheel loads. These cracks will then propagate through the week spots at the bottom of the asphalt layer, then they will propagate through the asphalt layer until they reach surface.

Cracking of Asphalt layer in flexible pavement is one of major source of distress in roadways. Combined vehicle and thermal load induced cracking in the forms of bottom-up fatigue cracking, reflective cracking and top-down fatigue cracking. A model that is able to simulate the initiation and propagation of cracks in asphalt layer is highly desirable. It will provide insights into these distress mechanisms and help improve mechanistic design procedures for cracks. For cracking problem, a natural solution would be to use fracture mechanics [**1]**. The single parameter could be either stress intensity factor K (or equivalently energy release G) or J-integral, depending on the size scale of the yielding in the material: the basis for the use of this approach is that the stress and strain field in the small zone ahead of the crack tip (called fracture process zone, or FPZ) in which fracture occurs is controlled by a signal parameter ,the stress intensity factor [**2]**.

Analysis of cracked asphalt pavement has been studied using the ABAQUS finite element computer program and show that the mechanism of crack failure was tension. Also the load position and base stiffness for flexible pavement affect on crack propagation and confirmed observation of crack growth in the field **[3]**.

In the asphalt concrete experimenting, notch specimens is often been adopted by the method of fracture mechanics, the shape of the notch is usually "U" or "V", and the testing means is bending or stretching. **[4]** presented a comprehensive research effort in which both traditional and new experimental protocols and analysis were applied to a laboratory

specimens and to field samples from pavements to determine the best combination of experimental work to improve the low temperature fracture resistance of asphalt pavement.

Definition of the traditional fatigue approach to pavement evaluation has been cited in some publications ***[5][6]***. The existing approach to performance prediction is broad and classifies pavement failure types that have been studied several times. The theories reviewed included the traditional fatigue approach, distortion energy approach, damage mechanics and fracture mechanics. Although it would possible to use any of the methods examined for predicting failure, it was determined that the combination of using finite element modeling and fracture mechanics was most appropriate for best analysis the behavior of crack growth and critical conditions at crack tip[7].

The primary objective of this research is to evaluate the fracture toughness and crack propagation. To accomplish the main objectives laboratory tests on fracture parameters of asphalt mixtures are made to evaluate the potential of stress intensity factor and fracture resistance of asphaltic materials. The linear elastic fracture mechanics used to determine crack propagation based on combined stress intensity factor due to dynamic cyclic load which may produce conditions that are favorable for fast fracture. Also investigate the stress states within the asphalt mixtures that influence the direction of crack propagation.

2. Fracture Mechanics

2.1 Mode of fracture

The separation or the fragmentation of a solid body into or more parts, under the action of stress is called fracture, figure (1). There are three independent kinematics movements of the upper and lower crack surfaces with respect to each other as shown in figure (2):

2. Opening Mode I: the two crack surfaces are pulled apart in the y-direction, but the deformations are symmetric about the xz and xy planes.
3. Shearing Mode II: the two crack surfaces slide over each other in the x-direction, but the deformations are symmetric about the xy plane and skew symmetric about the xz plane.
4. Tearing Mode III, the crack surfaces slide over each other in the z-direction, but the deformations are skewing symmetric about the xy and xz planes.

2.2 Stress Field in an Isotropic material in the vicinity of a crack tip

The stress components for the three fracture modes in an isotropic material are given next. In the case of anisotropic materials, these relations must be modified to permit the asymmetry of stress at the crack tip KI, KII, and KIII, respectively (the derivation of these expressions is to H.M. **Westergaard in 1939**.

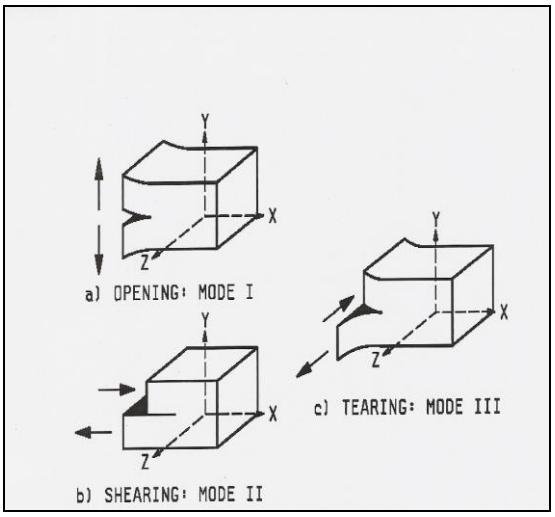

Figure (1): Independent Modes of Crack Displacements.

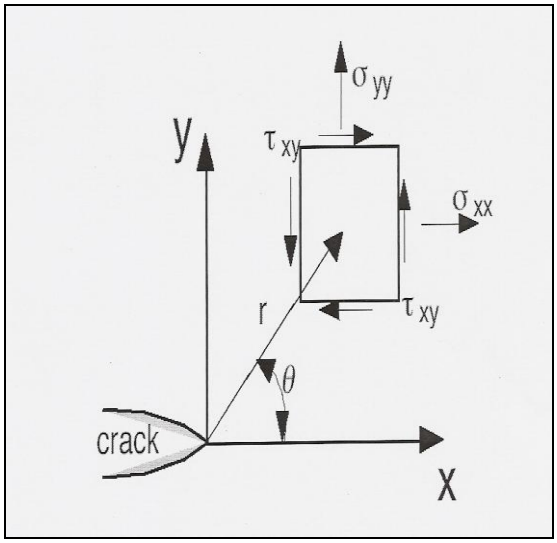

Figure (2): Polar Coordinates for the Crack Tip Region in the First Mode of Fracture.

Mode I:

$$\begin{bmatrix}\sigma_{11}\\ \sigma_{22}\\ \sigma_{12}\end{bmatrix}=\frac{K_I}{\sqrt{2\pi r}}\cos\frac{\theta}{2}\begin{bmatrix}1-\sin\frac{\theta}{2}\sin\frac{3\theta}{2}\\ 1+\sin\frac{\theta}{2}\sin\frac{3\theta}{2}\\ \sin\frac{\theta}{2}\cos\frac{3\theta}{2}\end{bmatrix} \quad \text{.....(1)}$$

Where:

$\sigma_{13}=\sigma_{23}=0$

$\sigma_{33}=0$ (plane stress)

$\sigma_{33}=\nu(\sigma_{11}+\sigma_{22})$ (plane strain)

Mode II:

$$\begin{bmatrix}\sigma_{11}\\ \sigma_{22}\\ \sigma_{12}\end{bmatrix}=\frac{K_{II}}{\sqrt{2\pi r}}\begin{bmatrix}-\sin\frac{\theta}{2}(2\cos\frac{\theta}{2})\\ \sin\frac{\theta}{2}\cos\frac{\theta}{2}\cos\frac{3\theta}{2}\\ \cos\frac{\theta}{2}(1-\sin\frac{\theta}{2}\sin)\end{bmatrix} \quad \text{..... (2)}$$

Where:

$\sigma_{13}=\sigma_{23}=0$

$\sigma_{33}=0$ (plane stress)

$\sigma_{33}=\nu(\sigma_{11}+\sigma_{22})$ (plane strain)

Mode III

$$\begin{bmatrix}\sigma_{13}\\ \sigma_{23}\end{bmatrix}=\frac{K_{III}}{\sqrt{2\pi r}}\begin{bmatrix}-\sin\frac{\theta}{2}\\ \cos\frac{\theta}{2}\end{bmatrix} \quad \text{..... (3)}$$

$$\sigma_{11}=\sigma_{22}=\sigma_{33}=\sigma_{12}=0$$

In this study, only KI is considered, the elastic corresponding displacement for plane strain is as follows ***[8]***:

$$u=\frac{K}{\mu}\sqrt{\frac{r}{2\pi}}\cos\frac{\theta}{2}\left(1-2\nu+\sin^2\frac{\theta}{2}\right) \quad \text{..... (4)}$$

$$v=\frac{K}{\mu}\sqrt{\frac{r}{2\pi}}\sin\frac{\theta}{2}\left(2-2\nu+\cos^2\frac{\theta}{2}\right) \quad \text{..... (5)}$$

While for plane stress

$$u=\frac{K}{\mu}\sqrt{\frac{r}{2\pi}}\cos\frac{\theta}{2}\left(\frac{1-\nu}{1+\nu}+\sin^2\frac{\theta}{2}\right) \quad \text{..... (6)}$$

$$v=\frac{K}{\mu}\sqrt{\frac{r}{2\pi}}\sin\frac{\theta}{2}\left(\frac{2}{1+\nu}+\cos^2\frac{\theta}{2}\right) \quad \text{..... (7)}$$

3. Stress Intensity Factor

In the linear elastic fracture mechanics (LEFM), the stress intensity in the field of the vicinity of crack in an opening mode is measured by means of a parameter known as the stress intensity factor, K_I. The stress intensity factor depends linearly on the applied stress and is a function of the geometry of the structure and the crack length. The theory of linear fracture mechanics is used to determine the fracture toughness in the materials and the main assumption of this approach is that the material behaves as a linear elastic solid. It was found ***[9]*** that this approach works well when inelastic behavior is observed near the region at the tip of a crack. For visco- elastic material such as HMA, this approach can be assumed valid if the zone of the plastic zone at the tip of the crack is small compared to the initial crack. in addition, the LEFM approach is only applicable for short term tests, not long tests such as creep tests.

For perfectly brittle material such as glass, there is no stable crack growth. The energy stored in the material in the vicinity of the crack is a function of the crack length, applied load, and the geometry of loading, it can be expressive using the stress intensity factorK_{IC}, which can also be related to the available energy for the propagation of the crack by a unit length. When the strain energy release rate is equal to the fracture toughness of the materialK_{IC}, the material fails by unstable propagation of the crack. Such a failure can be modeled based on LEFM principals using a single parameter, namelyK_{IC}.

For granular based material such as asphaltic concrete, crack growth is heterogeneous and tortuous; it is accompanied by aggregate interlock, micro cracking. Furthermore, the viscoelastic behavior results in the relaxation of stresses in the vicinity of the crack tip. These mechanisms give rise to a zone of nonlinear deformations generally referred to as the fracture process zone, resulting in the toughening of the material. ***[10]***.

4. Theoretical Formulation

It has been widely observed that fracture occurs in asphalt pavements mainly due to concentration of tensile stresses due to loads and or temperature variations. Thus the stress intensity factor in Mode I (K_{IC}) has been widely used to evaluate fracture toughness of asphalt mixtures. K_{IC} , generally determined by:

$$K_{IC} = \sqrt{E G_C} = \Upsilon \sigma_c \sqrt{\pi a} \quad \text{..... (8)}$$

where:

K_{IC}: critical stress intensity factor (Mode I).
E : elastic modulus.
G_C: critical strain energy release.
Y: numerical modification factor to account for crack geometry, loading conditions and edge effects.
σ_c: applied critical stress.
p : applied vertical load.
a : notch depth.

Therefore, 2 major factors affect the evaluation of the K_{IC} for (HMA), the geometry factor and the variation of elastic modulus of the mix under various conditions, especially temperature.

[11] developed equations for the Y factor for semi-circular sample under 3-point bending as shown in Figure (2), for different span ratios and different crack angles. Lims solution were verified by [***12]*** by using finite element and LFEM analysis. For span ratio (s/r) of 0.8, the factor Y can be determined using the following equation,

$$\mathrm{Y} = \mathrm{Y_I} + \frac{\Delta \mathrm{S_o}}{\mathrm{Y}} \mathrm{B} \quad \text{..... (9)}$$

where:

$\mathrm{Y_I}$: the normalized stress intensity factor.

$$\mathrm{Y_I} = 4.782 - 1.219 \left(\frac{\mathrm{r}}{\mathrm{a}}\right) + 0.063 \exp\left(7.045 \left(\frac{\mathrm{a}}{\mathrm{r}}\right)\right) \quad \text{..... (10)}$$

$\frac{\Delta \mathrm{S_o}}{\mathrm{Y}}$: deviation from actual span ratio of $\frac{s}{r} = 0.8$

B=6.55676+16.64035(a/r)^2.5+27.97042(a/r)^6.5+215.0839(a/r)^16, $0.003 \leq \mathrm{a/r} \leq 0.8$

r : sample radius.

Thus, for a SCNBF test K_{IC} can be determined as:

$$K_{IC} = \Upsilon \sigma_c \sqrt{\pi a} = \left(Y_I + \frac{\Delta s_o}{r} B\right) \sigma_c \sqrt{\pi a} \quad \text{..... (11)}$$

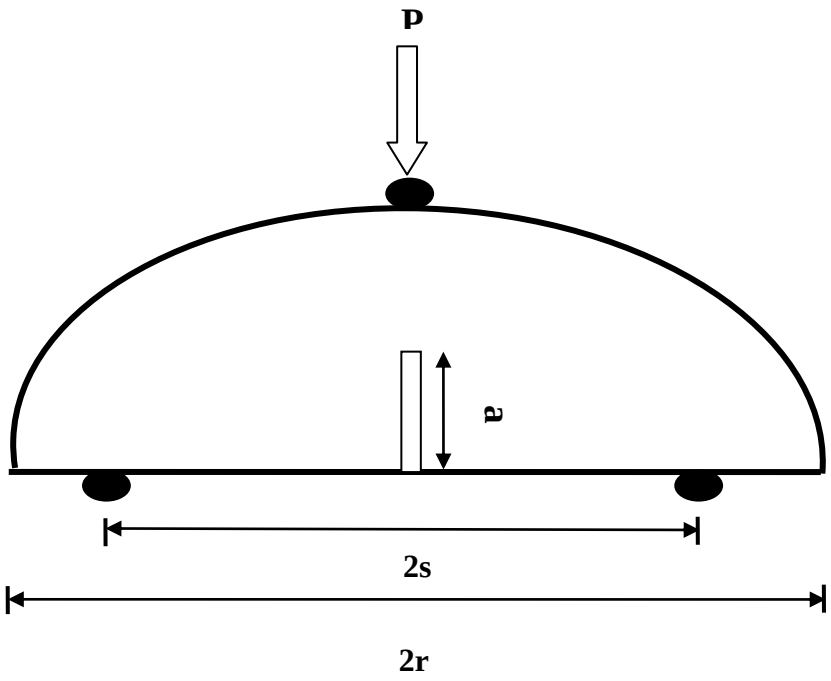

Figure (3): Semi Circular Bending Specimen (SCNB).

5. Experimental Testing

5.1 Materials

The materials used in this research are locally available and selected from currently local materials used in road construction in Iraq. The aggregate is brought from the hot mix of Al-Nibaee quarry at Al- Taji. The physical properties of coarse and fine aggregate are shown in Tables (1). The gradation of fine aggregate is passing No. 4 (4.75mm) and retained on No.200 (0.075). For the asphalt cement used in this research is brought from Al-Daurah Refinery. One type of asphalt cement is used in this study, (40-50) penetration grade. The physical properties for the asphalt cement used are presented in Table (2). The Portland cement is used as mineral filler and its chemical and physical properties are shown in Table (4).

Table 1: Physical Properties of Nibaee Aggregates.

Test Method	*Coarse Aggregate*	*Fine Aggregate*
Bulk Specific Gravity (ASTM C127 and C128)	**2.616**	**2.642**
Apparent Specific Gravity (ASTM C127 and C128)	**2.668**	**2.676**
Percent Water Absorption (ASTM)	**0.461**	**.628**
Percent Wear (Los Angeles Abrasion) (ASTM C131)	**22.27**	**……..**

Table 2: Physical Properties Asphalt cement.

Test	**Units**	**Penetration Grade (40-50)**	**Specification (SCRB)**
Penetration (25C^0, 100g, 5 sec.). ASTM-D5	**1/10 mm**	**44**	**40-50**
Ductility (25C^0, 5 cm/min). ASTM-D113	**cm**	**140**	**>100**
Softening Point (Ring and Ball). ASTM-D36	**C^0**	**49**	**54-60**
Specific Gravity at 25C^0. ASTM-D70	**…..**	**1.045**	
Flash Point 9Cleaved and open cup)ASTM-D92	**C^0**	**312**	**>232**
After Thin-Film Oven Test ASTM-D1754			
Penetration of Residue ASTM-D5	**1/10 mm**	**33**	
Ductility of Residue ASTM-D113	**cm**	**122**	
Loss in Weight (163 C^0 ,50gm, 5hr)	**%**	**0.175**	

Table 3: Physical properties of cement (mineral filler).

Specific Gravity	3.32
% Passing Sieve no. 200	92

5.2 Specimen preparation

Dried the aggregate of mix to a constant weight at 110 C^0, then the desired gradation is obtained by sieving to obtain the required gradation. The total weight of the mixture is approximately 1200gm with a specimen of 2.5 inch (63.5 mm) height by 4 inch (101 mm) diameter. Heating the aggregate and filler before mixing with asphalt to temperature of 160 C^0. Then the asphalt cement is heated on a hot plate to the temperature of 140 C^0 before mixing with aggregate. Finally after mixing all components the asphalt mixture is heated on a hot plate until it reaches a temperature of 140C^0 and keeping the temperature constant at (150-160 C^0). The temperature of mixing is maintained within the required limit (155-160 C^0).

5.3 Laboratory Test

5.3.1 Semi Circular bending Test

A schematic of semi circular bending test (SCB) set up is shown in Figure (4). A hydraulic testing machine system equipped with an environmental champer was used to perform the SCB test. The test was carried out at Ruhr University Bochum/ Department of Transportation Infrastructure (Lehrstuhl für Verkehrswegebau) /Germany, figure (5). The SCB samples were symmetrically supported by two fixed rollers and had a span of 120 mm as shown in Figure (2). The Marshall compacted cylindrical specimens were cut at the centerline using a water cooled circular saw with a diamond with cut depth and width (25 mm and 5mm) respectively. One of the specimens was left without a notch as a control specimen and the spacing between the 2- rollers supports was 120 mm. The test loading was performed by applying cyclic loading to the notched specimen at a constant rate of 0.5 mm/min and was carried out at two values of temperature ($20C^0$ and $0C^0$) . A digital controller was programmed to carry out all tests as shown in Figure (5), the load, deflection were continuously measured and recorded by a data acquisition system.

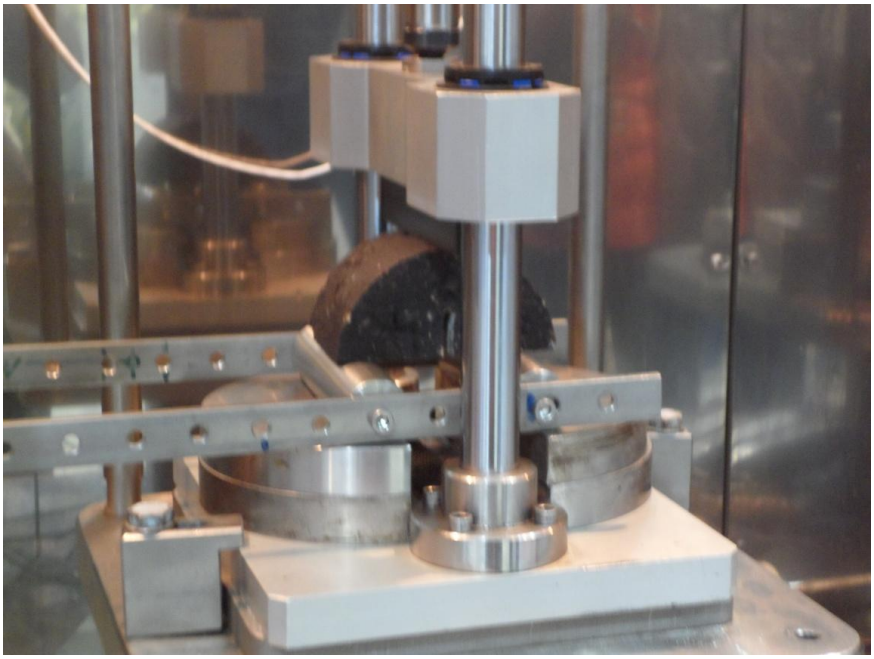

Figure 4: Semi Circular bending Test (SCNBT).

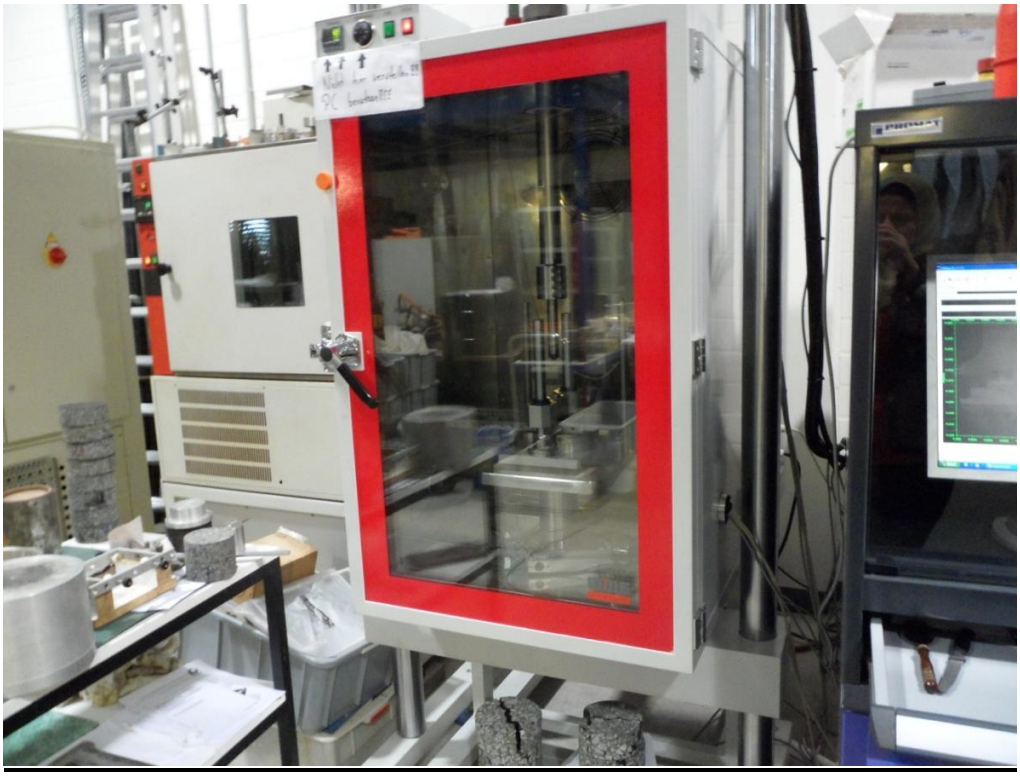

Figure 5: The Test Equipment and Instrument.

6. Experimental Results and Discussions

The semi circular bending test (SCB) was carried out at Ruhr University Bochum to investigate the resistance and crack propagation of asphalt mixtures. The fracture toughness (which has been computed from the peak load and specimen geometry of the material tested based on theory of fracture). Three levels of asphalt binder content were used (4, 5, 6) % for the asphalt concrete mixtures. All percentages were calculated by total weight of the mix and represented binder contents close to the optimum values for both types based on Marshall mix design. Two temperatures were used (0 C^o and 20 C^o).

The test was performed by applying a series of loading cycles to the notched semi circular specimen to obtain the load vs. displacement curve as shown in Figure (6) and (7) for 0 C^o and 20 C^o respectively. The fracture energy is a good indicator for determine the fracture resistance for asphalt mixture than other indicators such as tensile strength. It can be observed from these two figures that as the test temperature decrease (or get colder), the peak load increases and the total displacement decreases. The peak load increased by approximately (45.95 %) and the total displacement decreases by (19 %). Also Figure (8) shows the crack propagation during the test in front of the notch tip. It can be observed that fracture energy increases as the temperature increases. Since as the temperature increased the crack propagate around aggregate which increase the potential of aggregate interlocking and bridging. In lower Temperature the crack tend to propagate through both aggregate and binder resulting in decreasing the fracture energy or resistance of asphalt mixture as shown in Figure (9) and (10) for cracking propagation of the two specimen with different temperature (0 C^o and 20 C^o) respectively.

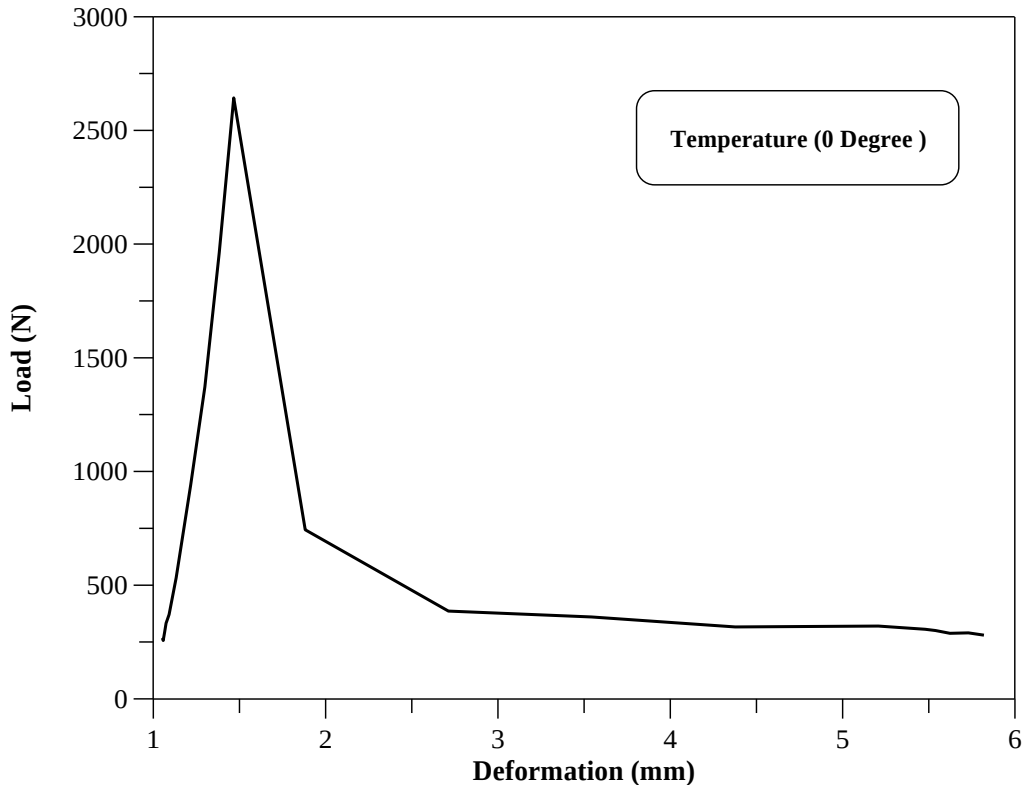

Figure 6: Experimental Load Deformation Curve during Fracture Test at $0C^0$ Temperature.

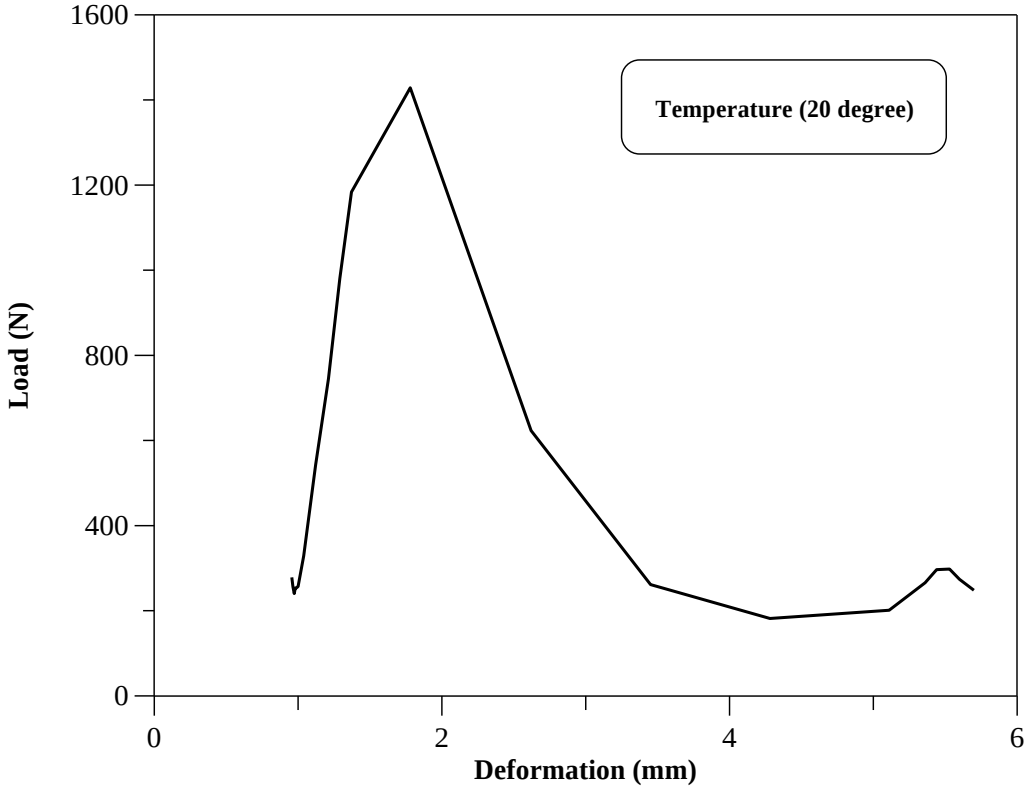

Figure 7: Experimental Load Deformation Curve during Fracture Test at $20C^0$ Temperature.

Figure 8: Crack Propagation during the Fracture Test.

Figure 9: Crack Propagation at Test Temperature $20C^0$.

Figure10: Crack Propagation at Test Temperature0C^0.

Figure (11) and (12) represents the variation of stress intensity factor with asphalt binder at two different test temperatures (0C^o and 20 C^o). Stress intensity factor K_{IC} critical stress intensity factor which is the stress intensity factor for an effective crack length at which unstable crack growth takes place. It can be noticed that the fracture toughness increased as the test temperature decreased, which means that the HMA becomes more brittle at cold temperatures. Also the asphalt mixture with 5% binder content at (0 C^o and 20 C^o) had the highest average K_{IC} (critical stress intensity factor) value. Decreasing test temperature increased the critical stress intensity factor by (57.5 %) . Again it can be concluded that as the temperature decrease, the fracture energy deceases as shown in Figure (6) and (7) but the fracture toughness increases as shown in Figure (11) and (12) respectively.

Figure (13) and (14) show the critical mouth opening displacement (CMOD), which is the crack opening at which the unstable crack growth takes place. It can notice from these two figures that decreasing the test temperature increase (CMOD). Also the asphalt mixture with (5%) binder had the lower critical mouth opening displacement CMOD at unstable crack. The failed specimens are shown in Figures (9) and (10) at two different test temperatures (20 C^o and 0C^o). Figures (15) and (16) show the variation of elastic modulus of asphalt mixture with binder content for different test temperature. The elastic modulus, (which is a measure of the stiffness of the material) is computed from the initial compliance of the specimen. It can be seen that increasing test temperature decreasing the stiffness modulus of (HMA) asphalt mixtures. The effect of asphalt binder is relatively caused slight decrease of the modulus as compared with temperature effects.

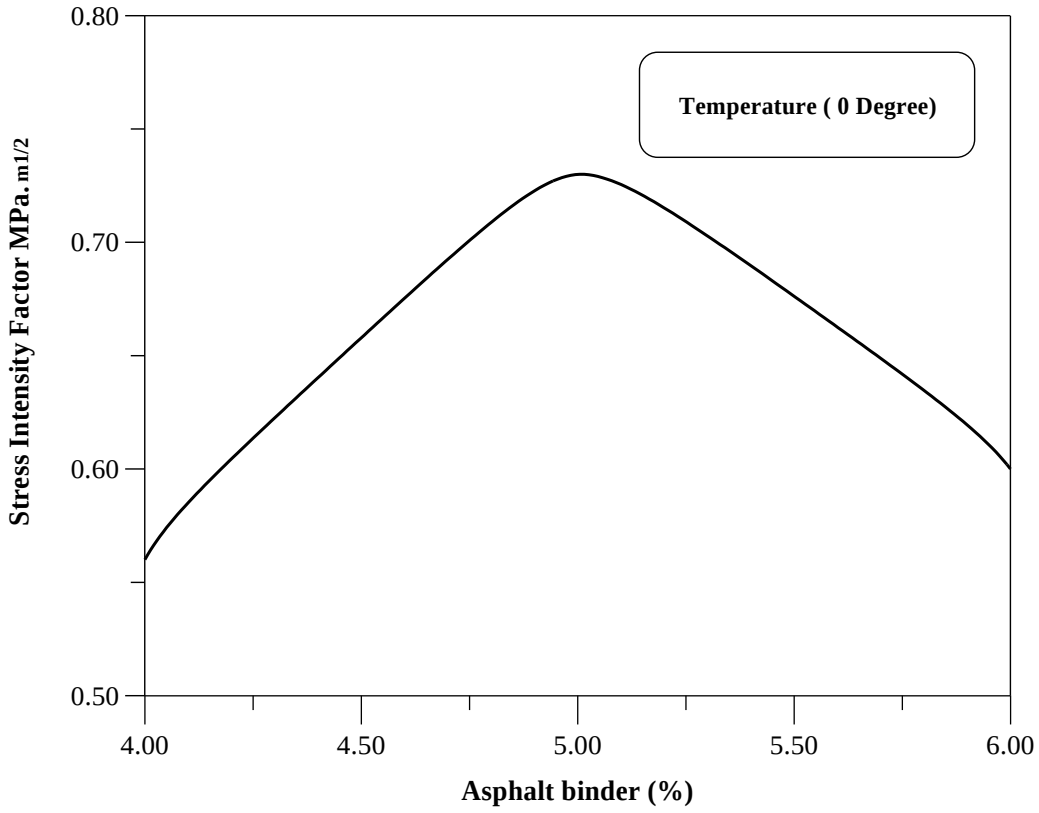

Figure 11: Variation of Stress Intensity Factor with Asphalt Binder at $0C^0$.

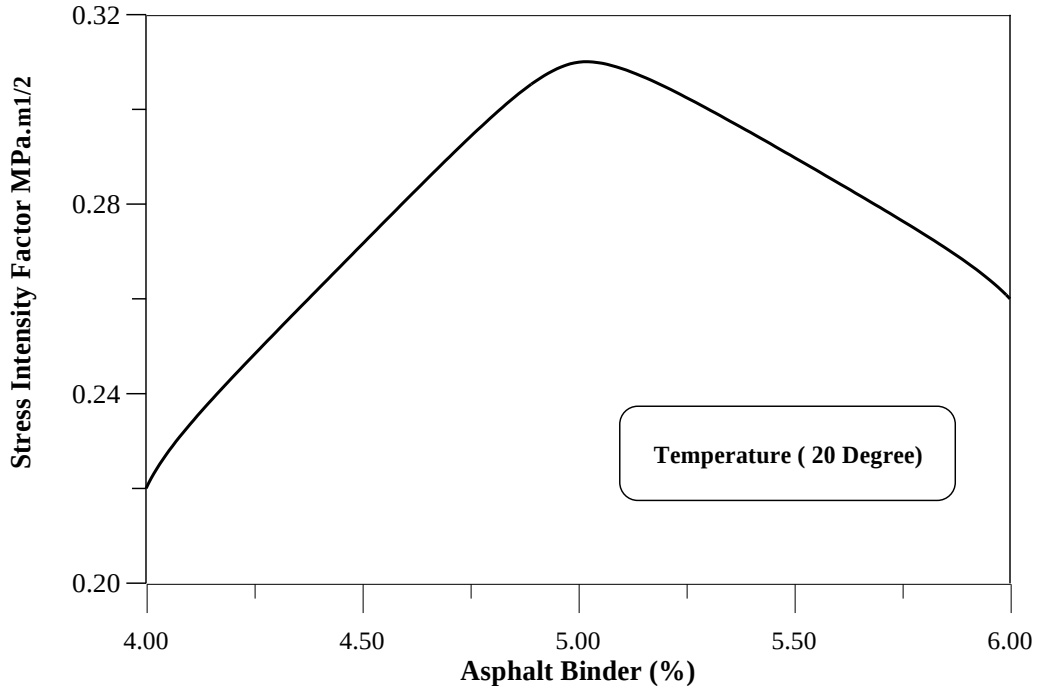

Figure 12: Variation of Stress Intensity Factor with Asphalt Binder at $20C^0$.

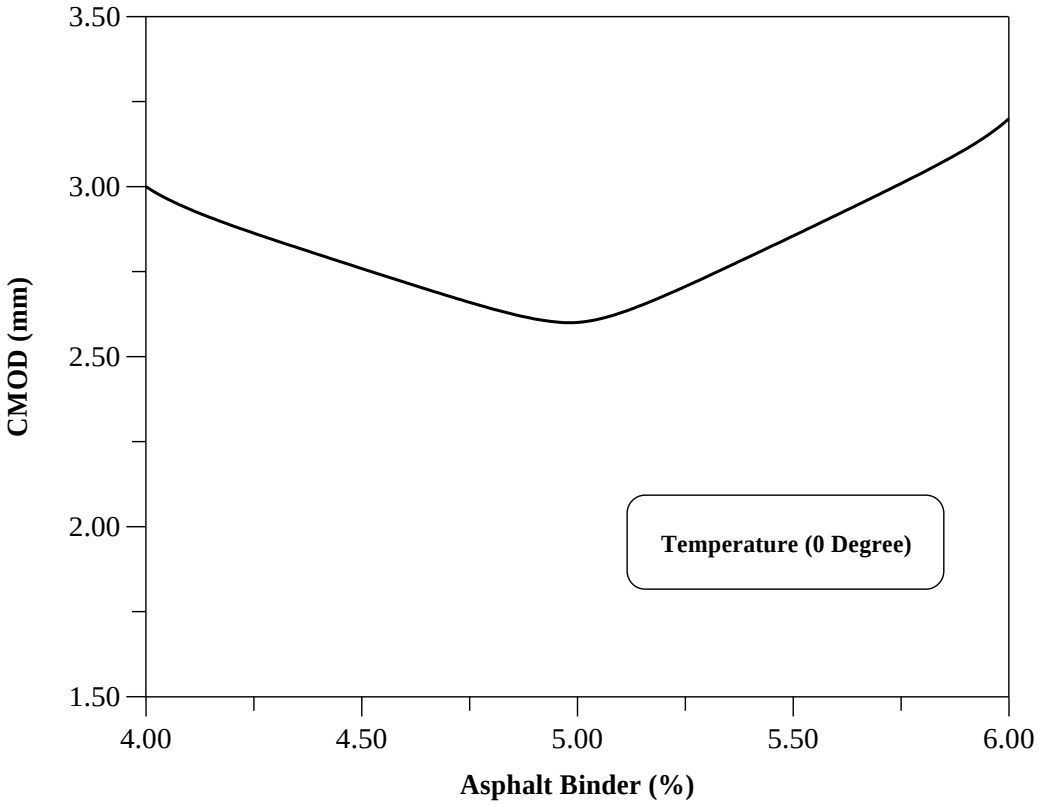

Figure (13): Variation of CMOD with asphalt Binder at $0C^0$.

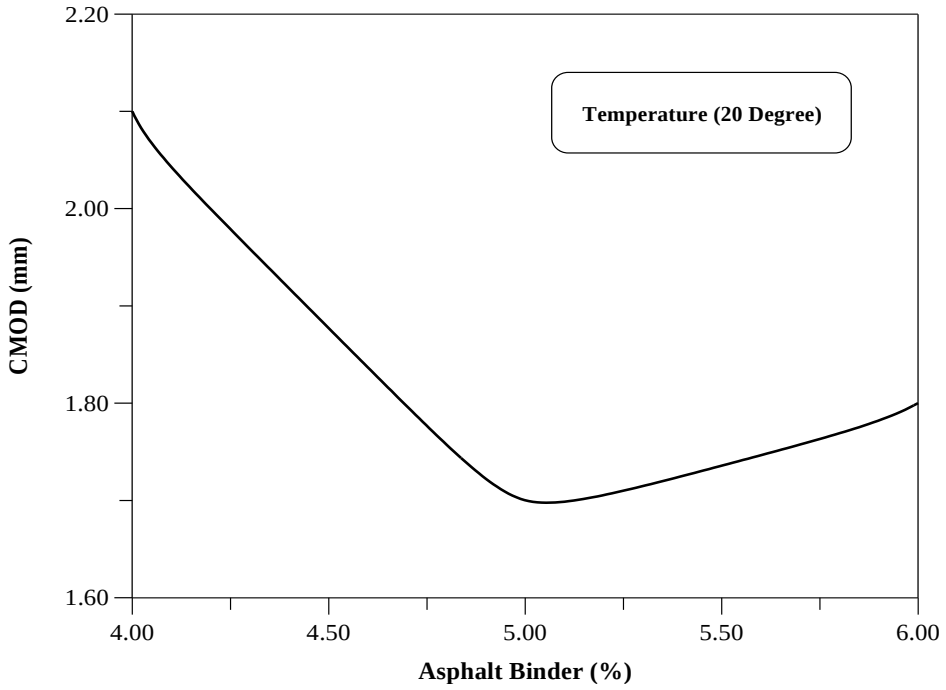

Figure14: Variation of CMOD with asphalt Binder at$20C^0$.

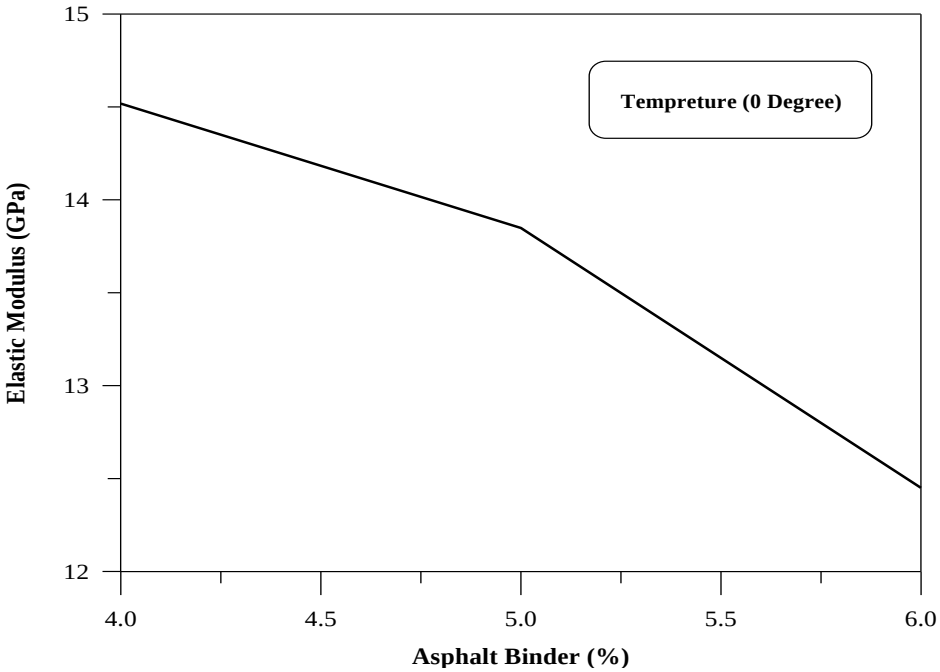

Figure (15): Variation of Stiffness Modulus of Asphalt Mixture at$0C^0$.

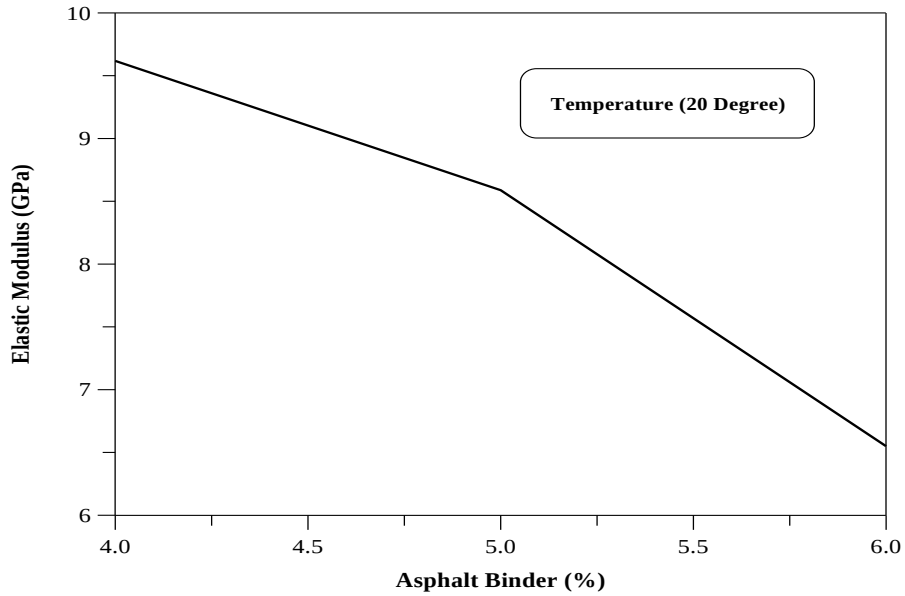

Figure (16): Variation of Stiffness Modulus of Asphalt Mixture at$20C^0$.

7. Finite Element Analysis

To further understand the behavior of fracture patterns and to verify the outcome of experimental test, the finite element program ANSYS (V.12.1) is used to evaluate the stress intensity factor based on numerical procedure. With the ANSYS (V12.1) finite element program simulation, numerical analysis can be utilized for the validation of the testing procedure. In this study the notched semi circular sample was modeled with ANSYS program in 3-Dimensional using solid 185 (8-node85) elements.

SOLID 185 is used for 3-dimensional modeling of solid structures. It is defined by eight nodes having three degree of freedom at each node: translations in the nodal x, y and z directions, and the element have plasticity, large deflection, large strain capability, creep and stress stiffening.

The model utilized the applied force to test the particles movement, deformation and stress distribution in a numerical simulation. The finite element working was carried out through generation of finite element mesh and defining load,

boundary conditions as shown in Figure (16). It is preferable to use finite element in places were high stress or strain gradients are expected, therefore the mesh consists of fine mesh close loaded area. Computing strains, stresses displacements and stress intensity factor and finally converted the obtained results into graphical outputs for ease understanding and discussions as shown in next section.

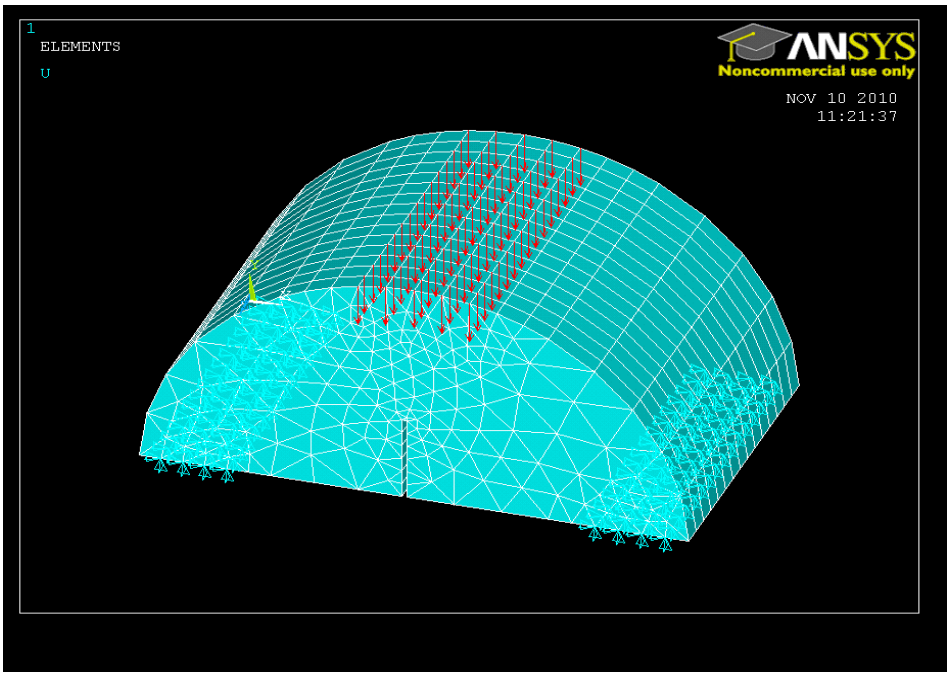

Figure (16): Finite Element Mesh and Boundary Conditions for Semi Circular Bending Test.

A comparisons are made with the values of Stress intensity factor obtained from fracture test and ANSYS program as shown in Figure (17) and (18) for different temperature (20 C^o and 0C^o) respectively. Also Figure (19) shows the comparison for the flow value results. The experimental results against which the Finite element model is compared are depicted by discrete lines. It can be seen from the figures that there is a good agreement between results of the finite element program and the measured one.

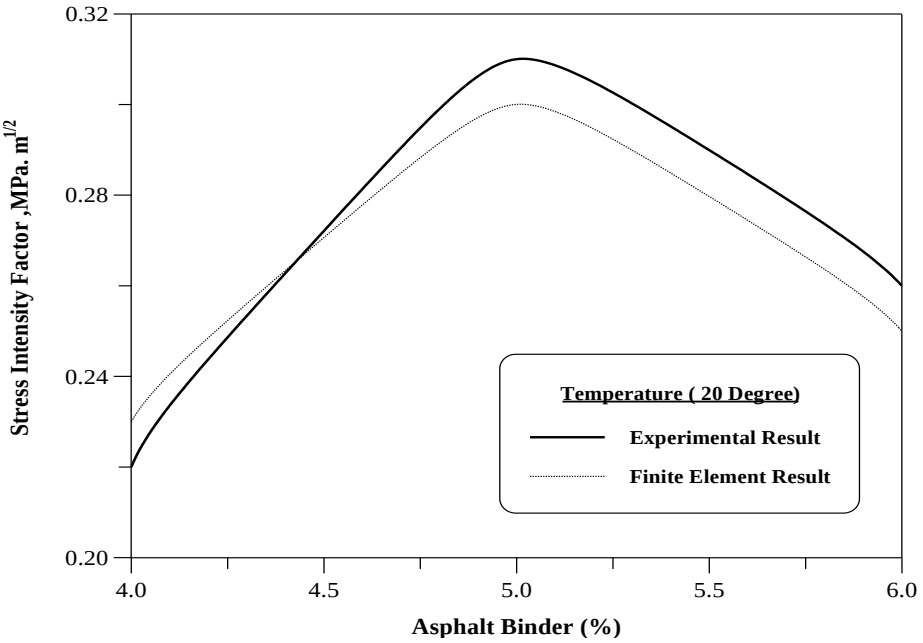

Figure 17: Variation of Stress Intensity Factor with Asphalt Binder at $20C^0$.

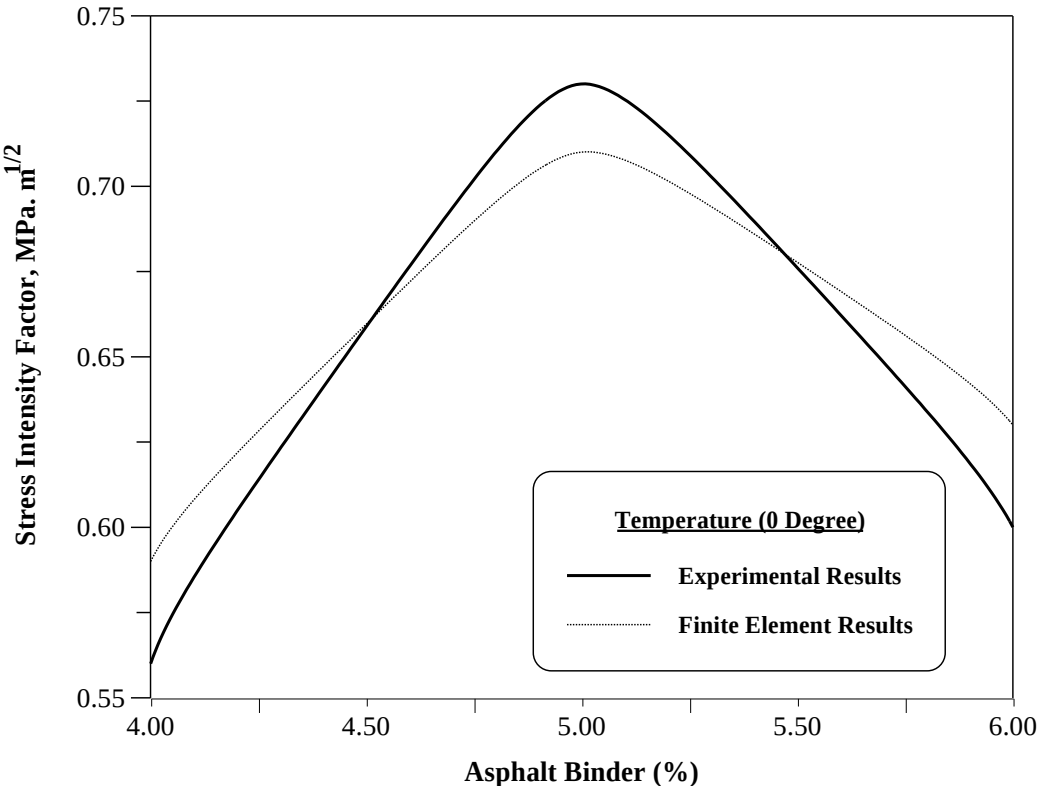

Figure (18): Variation of Stress Intensity Factor with Asphalt Binder at $0C^0$.

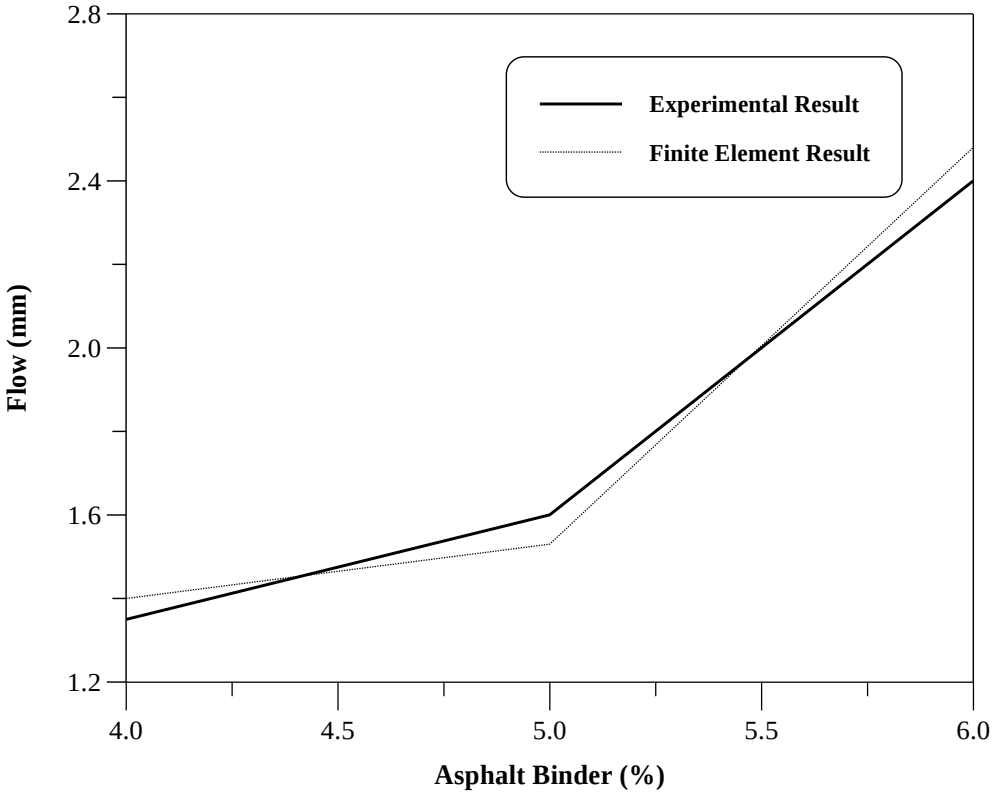

Figure (19): Comparisons of Flow Values of Different Asphalt Content with Finite Element Program Results.

Figure (20) to (25) show the deformation, strain and stress distribution within asphalt specimen during fracture test. Figure (20) and Figure (21) show the deformation in 2-D and 3-D view, it can be seen that maximum and critical deformation occurs under the loading area and near the zone of crack opening. Also critical deformation concentrate at top and propagate diagonally to the induced crack zone, which means that induced crack represent the weakest point as compared with the original specimen that remain without notch as shown in Figure (22) and (23).
It can be seen from the contour lines of horizontal strain distribution as shown in Figure (24), that maximum horizontal tensile strain starts from the crack notch tip and propagate upward, this means crack continue to propagate under the applied load from the area of crack notch. Also the maximum vertical compressive strain that occurs at the top of specimen under the applied load explained in Figure (25) help the crack propagation to reach the top then failure of specimen occurs as shown in Figure (26). The distribution of horizontal and vertical stresses also confirmed with the above results as shown in Figure (27) and (28) respectively.

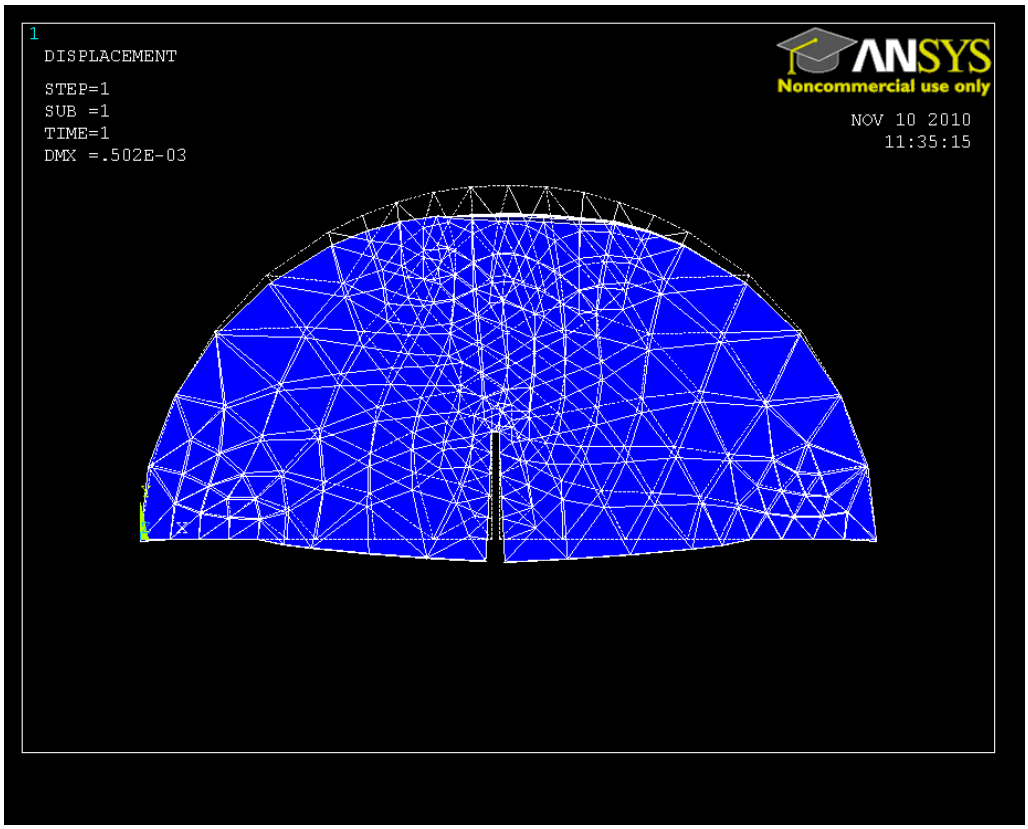

Figure 20: Deformation of SCNB specimen in 2-D View.

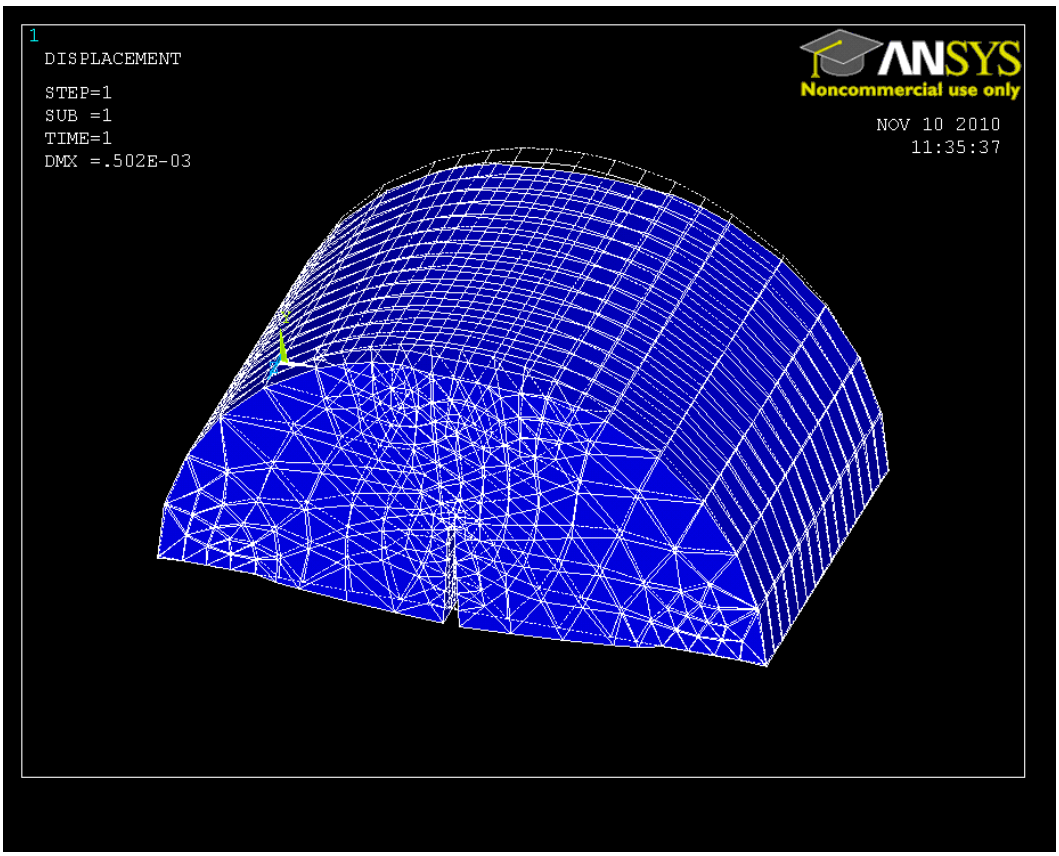

Figure 21: Deformation of SCNB Specimen in 3-D View.

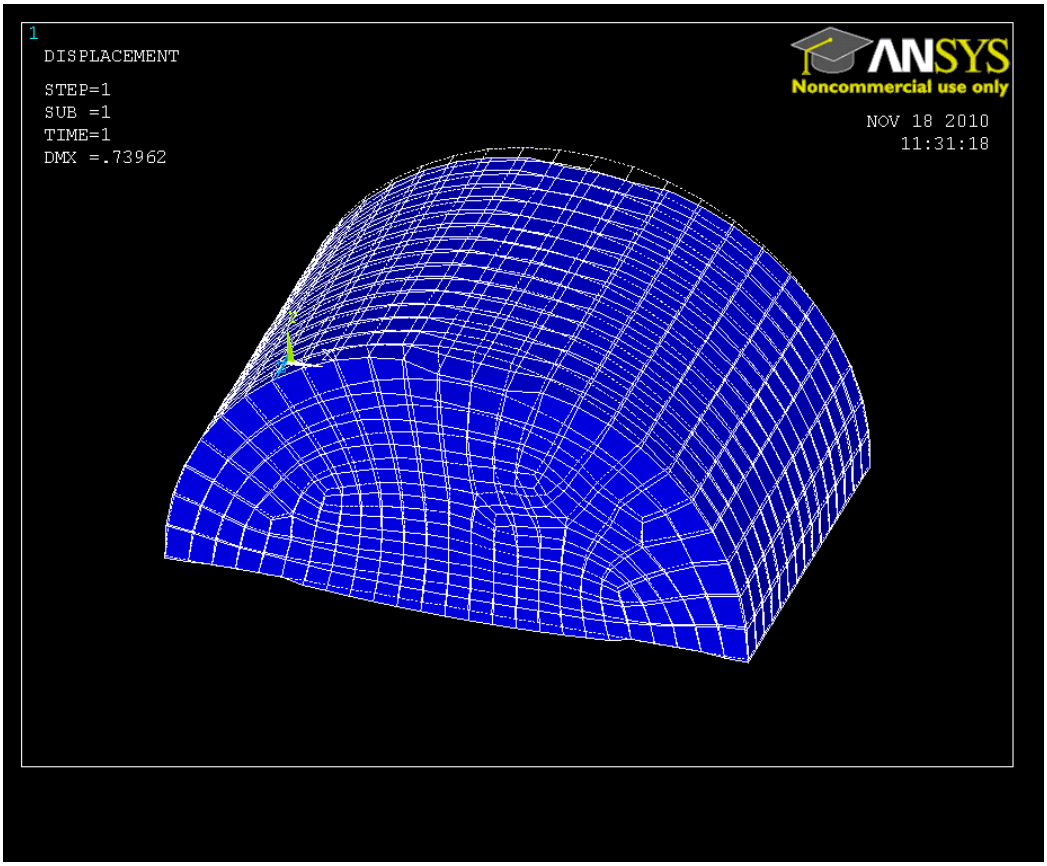

Figure (22): Deformation of SCB Specimen in 3-D View.

Figure (23): Failed SCB Specimen.

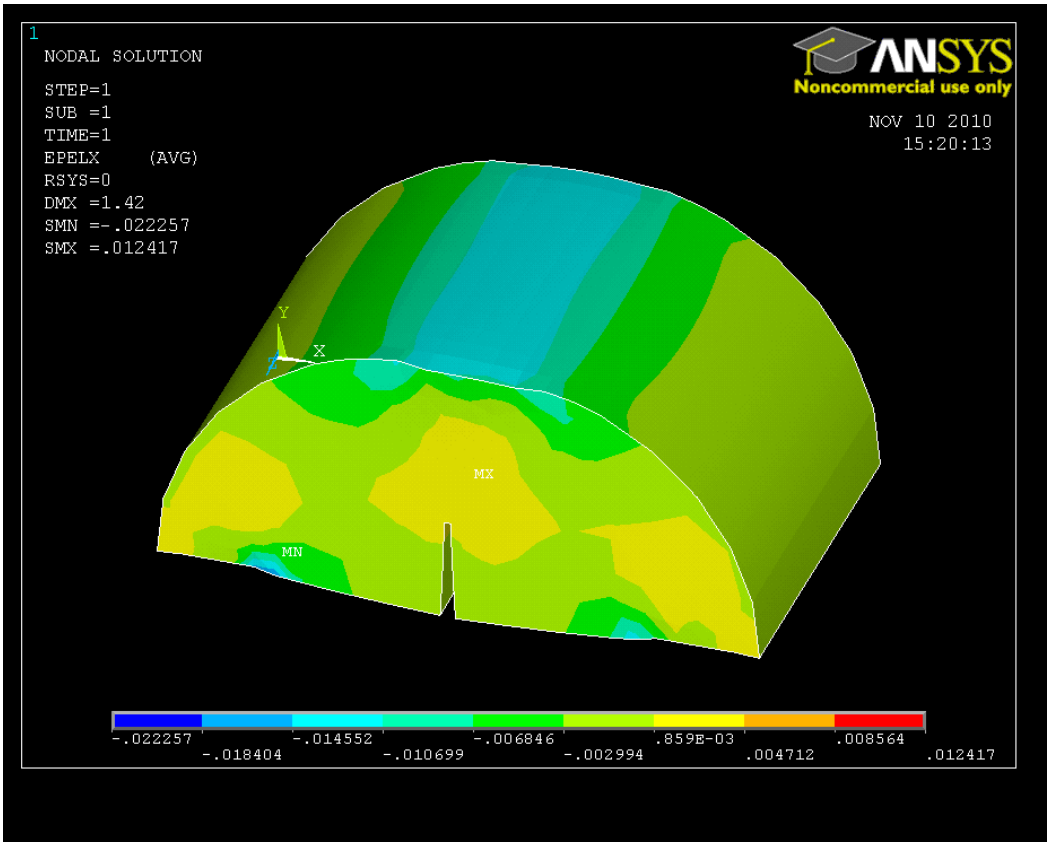

Figure 24:Horizontal Strain Distribution in SCNB Specimen.

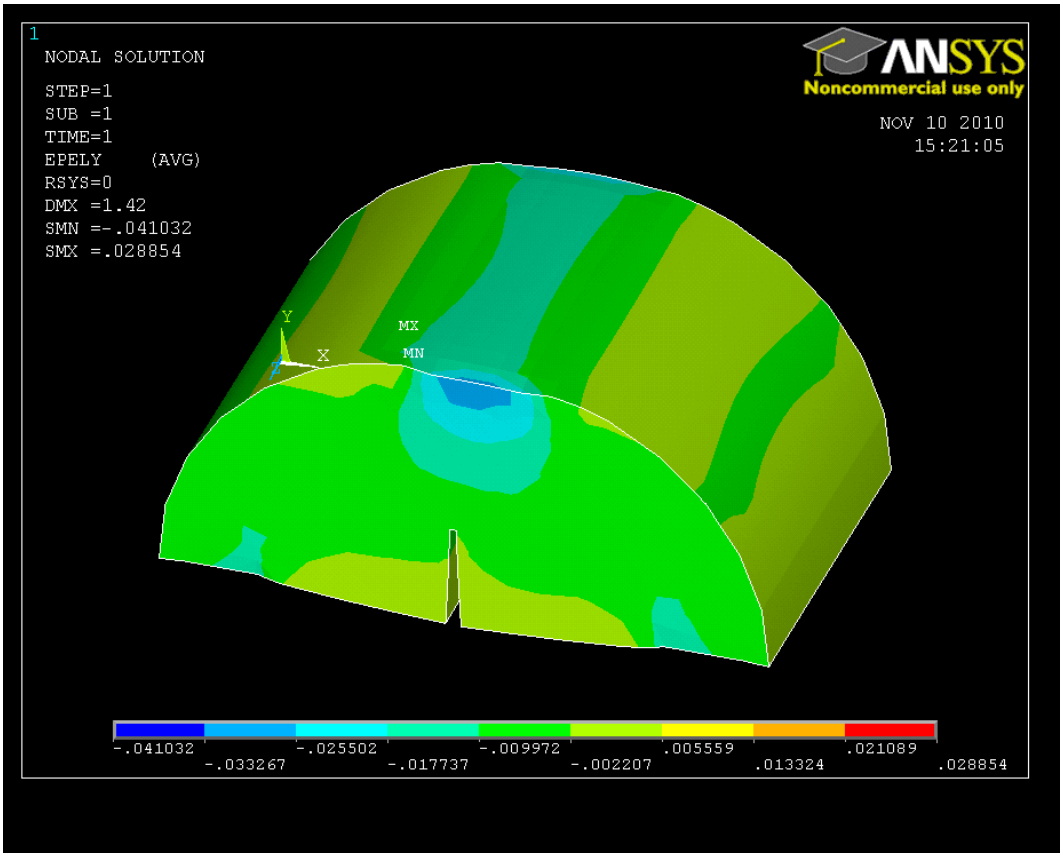

Figure 25:Vertical Strain Distribution in SCNB Specimen.

Figure 26: Failed SCNB Specimen.

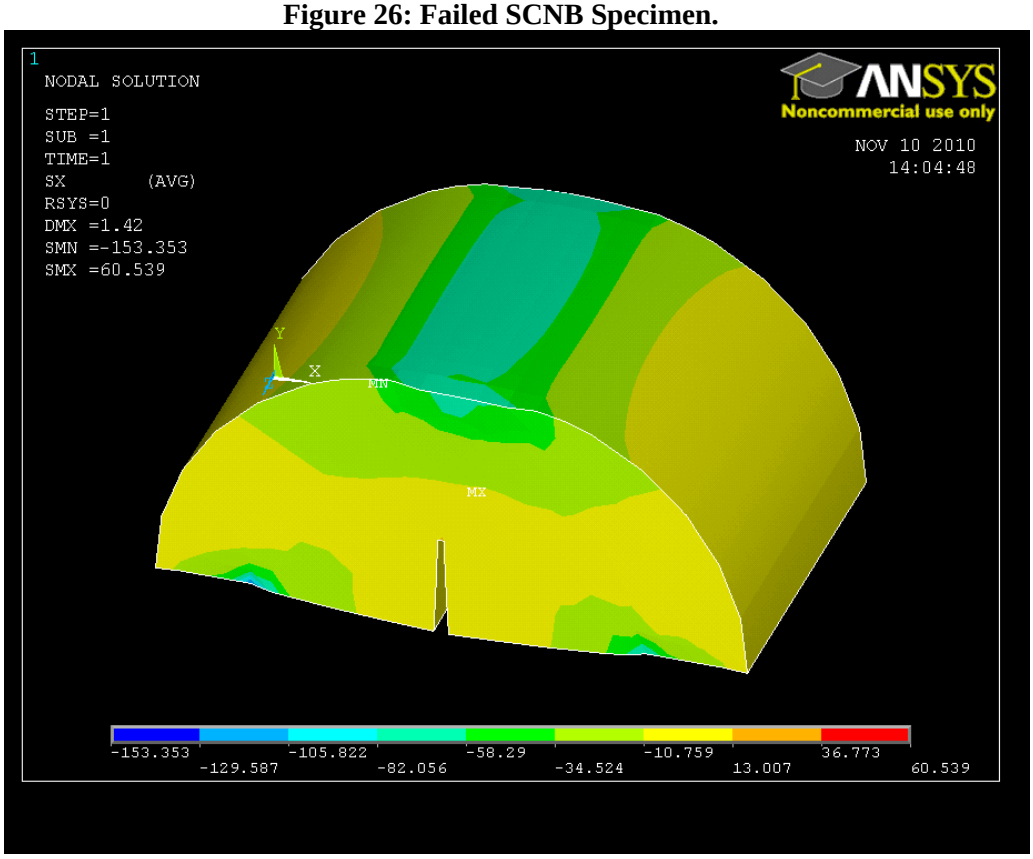

Figure 27: Horizontal Stress Distribution of SCNB Specimen.

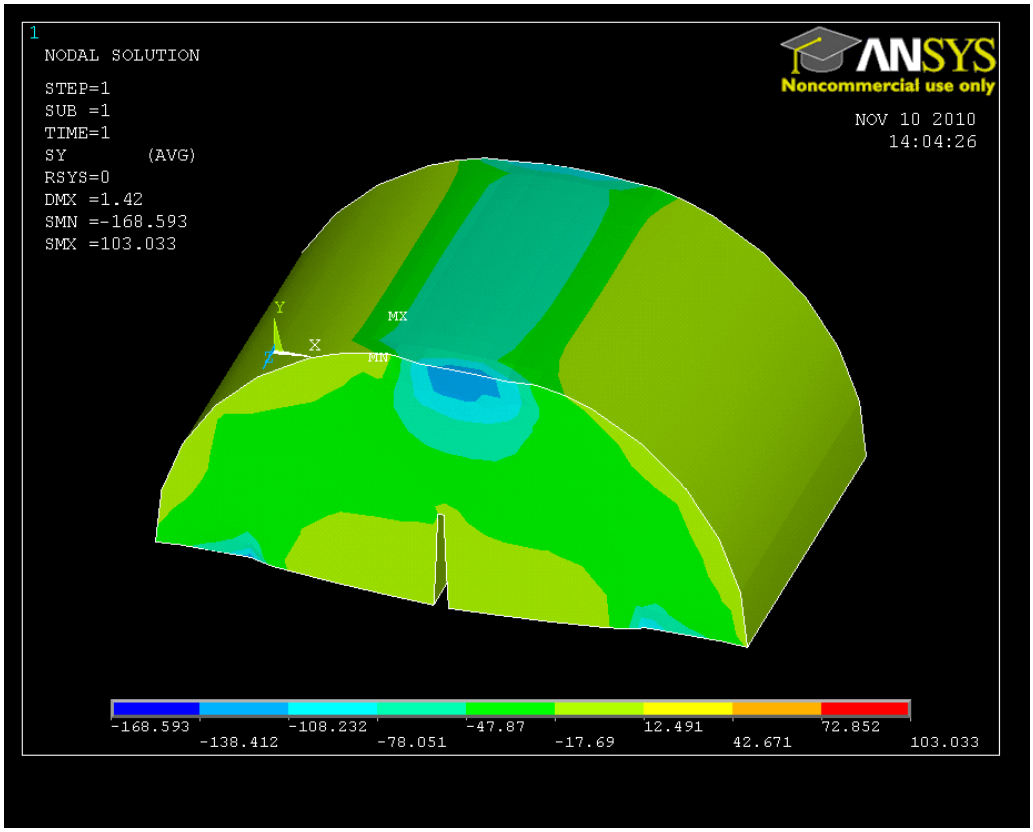

Figure 28: Vertical Stress Distribution of SCNB Specimen.

8. Conclusions

The main concluding remarks can be summarized as follows:

1. The fracture toughness increased as the test temperature decreased, which means that the HMA becomes more brittle at cold temperatures. Also the asphalt mixture with 5% binder content at (0 C^o and 20 C^o) had the highest average K_{IC} value. Decreasing test temperature increased the critical stress intensity factor by (57.5 %). Again it can be concluded that as the temperature decrease, the fracture energy deceases but the fracture toughness increases.
2. Decreasing the test temperature (or get colder), the peak load increases and the total displacement decreases. The peak load increased by approximately (45.95 %) and the total displacement decreases by (19 %). Also decreasing the test temperature increase the critical mouth opening displacement (CMOD). Also the asphalt mixture with (5%) binder had the lower critical mouth opening displacement CMOD at unstable crack.
3. The increasing in temperature lead to propagate of crack around aggregate which intern helps the potential of aggregate interlocking and bridging. In lower Temperature the crack tend to propagate through both aggregate and binder resulting in decreasing the fracture energy or resistance of asphalt mixture.
4. Increasing test temperature decreasing the stiffness modulus of (HMA) asphalt mixtures. The effect of asphalt binder is relatively caused slight decrease of the modulus as compared with temperature effects.
5. The maximum horizontal tensile strain starts from the crack notch tip and propagate upward, this means crack continue to propagate under the applied load from the area of crack notch. Also the maximum vertical compressive strain that occurs at the top of specimen under the applied load help the crack propagation to reach the top then failure of specimen occurs.

5. REFERENCES

[1] Anderson, T. **"**Fracture Mechanic: Fundamentals and Applications **"**, CRC Press, and 2nd Edition, Boca Raton, Fla. (1995)

[2] Canga, M. , Becker, E., and Ozupek, S, "*Constitutive Modeling of Viscoelastic Materials with Damage Computational* Aspects". Computer Methods in Applied Mechanics and Engineering, Vol.190, PP: 15-17. (2001).

[3] Leslie, A., Reynaldo, R. and Bjorn, B, "Propagation Mechanisms for Surface- Initiated Longitudinal Wheel Path Cracks". Paper Presented at the 80th Annual Meeting, TRB, Washington, D.C, USA, January 2001, 01-0433, (2001).

[4] Marasteanu M., et. Al, " Investigation of Low Temperature Cracking in Asphalt Pavements". Minnesota Department of Transportation, Research Services MS 330 /395 John Ireland Boulevard, (2007).

[5] Huang, H.Y, " Pavement Analysis and Design ". Prentice-HALL, Englewood Cliffs, New Jersey, (1993).

[6] Yoder, E. and Witczak, M., "Principles of Pavement Design". John Wiley and Sons, New York, (1975).

[7] Collop, A and Cebon, D, "A Theoretical Analysis of Fatigue Cracking in Flexible Pavements". Proceedings, Institution of Mechanical Engineers, Vol. 209, pp. 345-361, (1995).

[8] Aggarwal, S. and Nayak, G,"Elasto-Plastic Analysis as a Basic for Design of Cylinder Pressure Vessel with Different End Closures", Int. Journal of Pressure Vessel and Piping , Vol. 10, PP:271-269, (1982).

[9] Osswald, T. A. and G. Menges "Materials Science of Polymers for Engineers". 2nd edition, Cincinnati, Ohio: Hanser Gardner Publications Inc., (2003).

[10] Barzin and Mamlouk, M, " Cracking Resistance of Asphalt Rubber Mix Versus Hot Mix Asphalt". International Journal of Road Materials and Pavement Design, Vol. 5, No. 4, PP: 435-452, (2004).

[11] Lim et. al.," Stress Intensity Factor for Semi Circular Specimens under Three Point Bending". Engineering Fracture Mechanics, Vol. 44, No. 3, (1993).

[12] Li, X., and M. Marasteanu, "Evaluation of Low Temperature Fracture Resistance of Asphalt Mixture Using the Semi-Circular Bend Test". Journal of the Association of Asphalt Paving Technologists, Vol. 73, (2004): 401-426, (2004).